JOURNAL OF SOLID STATE CHEMISTRY **134,** 344–348 (1997)
ARTICLE NO. SC977577

An X-Ray and Electron Diffraction Study of the Intergrowth Tungsten Bronze $Sb_{0.16}WO_3$

S. T. Triantafyllou,* P. C. Christidis,*,[1] and Ch. B. Lioutas†

* *Department of Applied and Environmental Physics, Aristotle University of Thessaloniki, 54006 Thessaloniki, Greece; and*
† *Department of Solid State Physics, Aristotle University of Thessaloniki, 54006 Thessaloniki, Greece*

Received June 4, 1997; accepted July 29, 1997

The average structure of the orthorhombic antimony tungsten bronze, $Sb_{0.16}WO_3$, has been resolved by three-dimensional single-crystal X-ray diffraction (space group *Pmmm*, $a_{av} = 7.4261(7)$, $b_{av} = 10.2004(15)$, $c_{av} = 3.8061(7)$ Å, and $Z = 5$). The structure refinement based on 377 observed unique reflections with $I > 2\sigma(I)$ (3493 totally measured reflections) converged to $R = 0.064$. The structure is of the intergrowth tungsten bronze type (ITB), consisting of slabs of hexagonal tungsten bronze structure (HTB) interchanged with slabs of perovskite-like WO_3 structure (PTB) along [010]. The HTB slabs are one hexagonal tunnel thick and the PTB slabs are two WO_6 octahedra thick. The Sb atoms are distributed over two positions inside the hexagonal tunnels. Electron diffraction observations revealed a superstructure with $a_s = 2a_{av}$, $b_s = 2b_{av}$, and $c_s = 4c_{av}$, which may be attributed to an ordering of the Sb atoms. A possible structural model is proposed.

INTRODUCTION

Antimony tungsten bronzes, Sb_xWO_3, were first prepared and investigated by Parmentier *et al.* (1, 2) in a course of study of the systems Sb–*M*–O (*M* = Mo or W). They found that by direct reaction of Sb powder with WO_3 a number of perovskite-like phases appear in the following order as x increases from 0.01 to 0.07: one monoclinic, one orthorhombic, two tetragonal, and one cubic. For $x > 0.07$ a new orthorhombic phase of distinctly different structure type appears, together with the perovskite-like cubic phase. The new phase seems to form alone for compositions about $x = 0.15$, while for higher x values it coexists with metallic Sb. A first X-ray diffraction study on a sample of composition $Sb_{0.15}WO_3$ by the same authors (2) lead to orthorhombic symmetry with cell constants $a = 14.80$, $b = 20.37$, and $c = 15.15$ Å and possible space groups *Ibam* or *Iba*2. The structure has been initially considered as a superstructure ($4 \times 4 \times 5$) of the perovskite - like cubic $Sb_{0.07}WO_3$ ($a =$ 3.83 Å). An attempt, however, at that time to solve the structure from about 800 visually estimated intensities, recorded on Weissenberg photographs, failed. A later investigation by Ekström *et al.* (3) on the Sb_xWO_3 system using powder X-ray diffraction and electron microscopy methods revealed that in the composition range $0.12 < x < 0.20$ a series of structures appear, which can be regarded as more or less ordered intergrowths of lamellae of the perovskite-like WO_3 and hexagonal tungsten bronze structures. These authors were also able to propose a structural model for the ordered $Sb_{0.20}WO_3$ phase, in which single-raw hexagonal tunnels are intergrown with WO_3 slabs of two octahedra thick. The same structural model was also deduced by Dobson *et al.* (4) from high-resolution electron microscope images. However, possibly due to the scarcity of well-ordered single crystals, no structure refinement of this model from X-ray diffraction data has been reported so far. The present study has been undertaken with the aim to verify the proposed model from single-crystal X-ray and electron diffraction data and to elucidate some important structural aspects of the structure, as for example the distribution of the Sb atoms in the hexagonal tunnels and the appearance of the superstructure.

EXPERIMENTAL

Synthesis and Crystal Growth

Samples of nominal composition $Sb_{0.25}WO_3$ were prepared by heating mixtures of Sb and WO_3 powders in appropriate amounts at 1273 K for about 2 weeks in sealed evacuated silica tubes. This composition has been reported to be the most favorable for obtaining crystals with large, well-ordered regions (4).

X-Ray Diffraction

From powder X-ray diffraction patterns obtained with a modernized Philips PW 1050 diffractometer (Cu$K\alpha$ radiation, Si external standard) it was concluded that the phase

[1] To whom correspondence should be addressed.

0022-4596/97 $25.00

obtained was the same as that reported by Parmentier *et al.* (2) for the composition $Sb_{0.15}WO_3$. Using the cell constants given by these authors as starting parameters all the observed peaks could be readily indexed by a least-squares refinement (Table 1). The indices of all the observed reflections obeyed the conditions: $h = 2n$, $k = 2n$, and $l = 4n$, showing the existence of a substructure with cell constants $a_{av} = 1/2\ a_s$, $b_{av} = 1/2\ b_s$, and $c_{av} = 1/4\ c_s$, where the subscripts av stand for the subcell and the subscripts s stand for the supercell (cell given by Parmentier *et al.* (2)). For the single-crystal X-ray diffraction study, a number of crystals were first examined with the Buerger precession method, from which then a very small violet prism of dimensions $0.050 \times 0.020 \times 0.015$ mm was selected for the measurement of intensities. The single-crystal diffractometer used was a modernized Philips PW 1100. All measurements were performed using graphite monochromated Mo$K\alpha$ radiation and a scintillation counter. The reflection search routine of the diffractometer led to an orthorhombic P lattice with parameters a_{av}, b_{av}, and c_{av} related to those given by Parmentier *et al.* (2) by $a_{av} = 1/2a_s$, $b_{av} = 1/2b_s$, and $c_{av} = 1/4c_s$, in agreement with the powder pattern findings. It should be noted, however, that in terms of these subcell axes only reflections with $h_{av} = 2n$ had appreciable intensities. Accurate cell parameters were obtained by a least-squares fit of the accurate 2θ values of 31 reflections in the region $15.89^\circ < 2\theta < 31.02^\circ$ and are given along with other crystallographic data in Table 2. Intensity data were collected for one hemispere of the reciprocal lattice in the region $3^\circ < 2\theta < 55^\circ$ (scintillation counter, $2\theta/\omega$ scans, 50 steps/reflection increased for $\alpha_1 - \alpha_2$ splitting, step width 0.02°, 0.5–2 s/step, 3 standard reflections every 120 min). A total of 3493 reflections (excluding standards) were measured, which were further corrected for Lorentz, polarization, and absorption (ψ-scans technique) effects. No systematic extinctions were found, thus leading to *Pmmm*, *Pmm*2, and *P*222 as possible space groups. By merging the symmetry equivalent reflections, a set of 428 unique reflections were obtained of which 377 were considered as observed [$I > 2\sigma(I)$] and included in the ensuing calculations. The internal agreement factor of the intensities was $R_{int} = 0.09$.

TABLE 2
Crystallographic Data for $Sb_{0.16}WO_3$

	Average structure	Superstructure	
	This study	This study	Parmentier *et al.* (2)
Space group	*Pmmm*	—	*Ibam* or *Iba*2
a (Å)	7.4261(7)	14.8521(14)	14.80
b (Å)	10.2004(15)	20.4008(30)	20.37
c (Å)	3.8061(7)	15.2244(29)	15.15
V (Å^3)	288.31(7)	4613(1)	4567.36
Z	5	80	80
$F(000)$	530.8	8492.8	
ρ_{cal} (gr cm^{-3})	7.238	7.238	
μ(Mo$K\alpha$) (cm^{-1})	544.8	544.8	

For the crystal structure analysis calculations the XTAL system of programs was used (5). Atomic scattering factors for neutral atoms and anomalous dispersion corrections were taken from Ref. (6). For the structure solution and refinement the space group *Pmmm* was initially adopted taking into account that the intensity statistics clearly favored a centrosymmetric space group. The positions of the W atoms were derived from a sharpened Patterson map, while the positions of the remaining atoms were obtained from a difference Fourier map, computed with the refined positions of the W atoms alone. The two highest symmetrical peaks (Fig. 1) observed at the position x, 0, 1/2 (point

TABLE 1
Observed and Calculated Values of *d* Spacings, Observed Intensities, and Indices for the Reflections of a Sample of Overall Composition $Sb_{0.25}WO_3$ [$a = 14.838(5)$, $b = 20.388(7)$, $c = 15.206(7)$ Å]

d_{obs}	d_{cal}	I_{obs}	h	k	l	d_{obs}	d_{cal}	I_{obs}	h	k	l
10.178	10.194	3	0	2	0	2.508	2.506	4	4	6	0
7.406	7.419	4	2	0	0	2.356	2.355	5	4	4	4
6.005	5.999	3	2	2	0	2.039	2.039	7	0	10	0
5.098	5.097	13	0	4	0	1.901	1.901	6	0	0	8
4.203	4.201	2	2	4	0	1.855	1.855	4	8	0	0
3.800	3.802	23	0	0	4	1.839	1.839	3	4	8	4
3.709	3.710	9	4	0	0	1.787	1.787	7	4	10	0
3.483	3.486	13	4	2	0	1.743	1.743	3	8	4	0
3.397	3.398	100	0	6	0	1.699	1.699	13	0	12	0
2.998	2.999	10	4	4	0	1.667	1.667	5	8	0	4
2.655	2.655	4	4	0	4	1.627	1.628	4	8	6	0
2.569	2.569	5	4	2	4	1.617	1.617	4	4	10	4
2.533	2.534	9	0	6	4	1.551	1.551	4	0	12	4

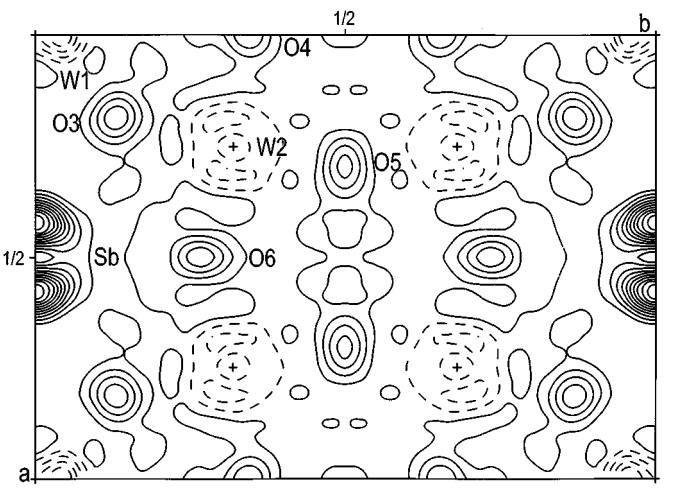

FIG. 1. Difference Fourier section at $z = 1/2$ computed with only the tungsten atoms. Their positions are indicated by small crosses. The two most prominent peaks of the map at the position x, 0, 1/2 are assigned to a disordered Sb atom. Contours are at 5.0 e Å^{-3} intervals.

group symmetry: 2*mm*) were assigned to the Sb atom, for which a statistical distribution over these two sites was assumed. The atomic positions were first refined isotropically, using unit weights and a variable occupation factor for the Sb atom. In the final stage of refinement (full matrix based on *F*'s) anisotropic displacement parameters were introduced for the W and Sb atoms. Moreover, an isotropic extinction correction (crystal type 2, Lorentzian distribution (7a, 7b)) and a weighting scheme of the form $w^{-1} = \sigma^2(F_o) = \sigma^2(F_o)_{\text{statistics}} + \sigma^2(F_o)_{\text{mod}}$, where $\sigma^2(F_o)_{\text{mod}}$ is the so called "ignorance factor" (5), were applied. The refinement results after convergence was reached were $R = 0.064$, $R_w = 0.083$, $GOF = 1.05$, and $[\Delta p/\sigma(p)]_{\max} = 0.48$. The residual electron density extrema were found near the *W* positions with heights about 1/3 of the height of an oxygen peak. Atomic positional and displacement parameters of the average structure are given in Table 3. After completion of the least-squares refinement in the space group *Pmmm* the acentric space groups *Pmm*2 and *P*222 were also tested. The obtained *R* values, however, did not improve significantly according to the Hamilton's $\mathcal{R}$ ratio test (8). Hence the space group *Pmmm* was retained to describe the average structure of the studied crystal.

Electron Diffraction

The electron diffraction study was performed using finely crushed particles of the bulk material glued on copper grids on a JEOL 120CX microscope operating at 120 kV.

RESULTS AND DISCUSSION

The Average X-Ray Structure

A normal projection of the structure along the **c** axis is shown in Fig. 3. Selected bond lengths and angles are shown in Table 4. The present study confirmed the structural model proposed by Ekström *et al.* (3) from a high-resolution electron microscopy study for the phase $Sb_{0.20}WO_3$. The structure is of the intergrowth tungsten bronze (ITB) type characterized by thin slabs of hexagonal tungsten bronze (HTB) structure, which are interchanged with slabs of perovskite-like WO_3 slabs (PTB) along [010]. The (HTB) slabs are one hexagonal tunnel thick and the WO_3 slabs are two WO_6 octahedra thick. This ITB structure type may be designated as (2) according to the notation proposed by Hussain and Kihlborg (9).

There are two symmetrically independent WO_6 octahedra in the structure. The first octahedron with the central W atom at the position 0, 0, 1/2 has the point group symmetry *mmm*, while the second octahedron with the W atom at the position *x*, *y*, 1/2 has the point group symmetry *m*. As a consequence, the first octahedron appears more regular, having all its W–O distances equal within the experimental error [$\langle$W–O$\rangle$ = 1.91(2) Å] and showing a maximum O–W–O angle deviation of 2.2(8)° from the ideal value of 90°. The vertical W–O axis in this octahedron is forced by symmetry to be parallel to the **c** axis. In the second octahedron, the W–O distances range between 1.876(6) and 1.989(19) Å [$\langle$W–O$\rangle$ = 1.918(4) Å], while the

TABLE 3
Atomic Positional, Displacement, and Site Occupation Parameters for the Structure of $Sb_{0.16}WO_3$

Atom	*x*	*y*	*z*	*U* or U_{eq}	*pp*
W1	0	0	1/2	0.0236(7)[a]	1
W2	0.2509(1)	0.31963(9)	1/2	0.0169(5)[a]	1
Sb	0.426(1)	0	1/2	0.039(3)	0.393(9)
O1	0	0	0	0.03(1)	1
O2	0.254(2)	0.315(1)	0	0.008(4)	1
O3	0.186(2)	0.130(2)	1/2	0.016(3)	1
O4	0	0.353(3)	1/2	0.027(6)	1
O5	0.300(4)	1/2	1/2	0.021(5)	1
O6	1/2	0.261(3)	1/2	0.026(6)	1

Atomic anisotropic displacement parameters

Atom	U_{11}	U_{22}	U_{33}	U_{12}	U_{13}	U_{23}
W1	0.027(1)	0.004(1)	0.039(1)	0	0	0
W2	0.0093(8)	0.0098(8)	0.0316(9)	−0.0003(3)	0	0
Sb	0.013(3)	0.080(7)	0.023(4)	0	0	0

[a] Denotes equivalent isotropic displacement parameters.

$$U_{eq} = \frac{1}{3}\sum_i \sum_j U_{ij} a_i^* a_j^* \mathbf{a_i} \cdot \mathbf{a_j}.$$

TABLE 4
Selected Interatomic Distances (Å) and Bond Angles (°) for the Structure of $Sb_{0.16}WO_3$

		Symmetry			Symmetry
W1–O1	1.9031(3)	(1, 1)	W2–O4	1.894(6)	(1, 1)
–O1	1.9031(3)	(1, 5)	–O5	1.876(6)	(1, 1)
–O3	1.92(2)	(1, 1)	–O6	1.943(9)	(1, 1)
–O3	1.92(2)	(1, 2)	Sb–O3	2.22(2)	(1, 1)
–O3	1.92(2)	(1, 6)	–O3	2.22(2)	(1, 6)
–O3	1.92(2)	(1, 7)	–O3	3.17(2)	(1, 8)
W2–O2	1.9037(5)	(1, 1)	–O3	3.17(2)	(1, 9)
–O2	1.9037(5)	(1, 5)	–O6	2.72(3)	(1, 1)
–O3	1.99(2)	(1, 1)	–O6	2.72(3)	(1, 8)
O1–W1–O3	90	(1, 1, 1)	O2–W2–O6	89.0(4)	(1, 1, 1)
O3–W1–O3	87.8(8)	(1, 1, 6)	O3–W2–O4	86(1)	(1, 1, 1)
O3–W1–O3	92.2(8)	(1, 1, 7)	O3–W2–O6	86(1)	(1, 1, 1)
O2–W2–O3	88.9(4)	(1, 1, 1)	O4–W2–O5	91(1)	(1, 1, 1)
O2–W2–O4	90.9(4)	(1, 1, 1)	O5–W2–O6	97(1)	(1, 1, 1)
O2–W2–O5	91.2(4)	(1, 1, 1)			

Note. Symmetry codes:

1: *x*, *y*, *z*	4: $-x, y, -z$	7: $-x, y, 1-z$
2: $-x, -y, z$	5: $x, y, 1+z$	8: $1-x, -y, z$
3: $x, -y, -z$	6: $x, -y, 1-z$	9: $1-x, y, 1-z$.

maximum O–W–O angle deviation from the ideal 90° value is 7(1)°. Moreover, the vertical W–O axis of the octahedron is slightly inclined with respect to the structure's **c** axis [1.5(4)°].

As stated earlier, the Sb atom with ideal position at the centre of the hexagonal tunnel (1/2, 0, 1/2) is split over two sites along [1 0 0], the distance between them being 1.098 Å. For the average structure a random distribution of the Sb atom over these two sites was assumed, implying a site occupation factor 0.5 for both of them, if all the hexagonal tunnels were filed with Sb atoms. The stoichiometry of the sample in this case would be $Sb_{0.20}WO_3$, which corresponds to the richest composition in Sb content. However, the least-squares refinement resulted in a site occupation factor for the Sb atom equal to 0.393 (9) (Table 3), which implies a composition $Sb_{0.16\pm1}WO_3$ for the studied crystal. The result explains the fact that traces of metallic antimony were observed at the ends of the silica tube during the preparation of the sample.

Concerning the Sb–O distances on the plane $z = 1/2$, two of them appear short and four long, as a result of the Sb splitting. While the two short Sb–O distances [2.22(2) Å] are in good agreement with the sum of the ionic radii for Sb^{3+} and O^{2-} (2.16 Å) (10), the long Sb–O distances, which range between 2.72(3) and 3.17(2) Å, are considerably larger. The off-center displacement of the Sb atom normally to the tunnel axis may be attributed to the stereoactivity of the $5s^2$ lone pair of the Sb^{3+} ion, which should be directed along [100] in our case. Similar situations have been observed in many bronzes and other related compounds, where the inserted metal ions possess outer electron lone pairs, e.g., in $In_{0.30}WO_3$ and $Tl_{0.30}WO_3$ (11), $Sn_{0.30}WO_3$ (12) and $Pb_{0.26}WO_3$ (13).

The Superstructure

Electron diffraction (ED) observations performed on the bulk material grains revealed an orthorhombic reciprocal space. Figure 2 shows the most informative ED patterns obtained from the tilting experiments. The lattice parameters deduced for the superstructure cell are $a_s = 14.98$, $b_s = 20.55$, $c_s = 15.30$ in very good agreement with the XRD results. The main features of ED patterns along the [010] zone axis (Fig. 2a) are: (a) $h0l$ reflections with $h = 2n$ and $l = 4n$ are much more stronger than the other reflections. Consequently, it is very difficult to detect reflections of the latter type by XRD experiments. (b) There is a set of very weak reflections with h, $l = 2n + 1$ that is consistent with the general condition $h + k + l = 2n$. This type, however, violates the special condition $h0l$: $h = 2n$ reported in Ref. (2). (c) There is a second set of even weaker reflections, indicated by small arrows, which violate the reflection condition $h + k + l = 2n$. Reflections of this type are present in all ED patterns. However, they may be interpreted as a result of

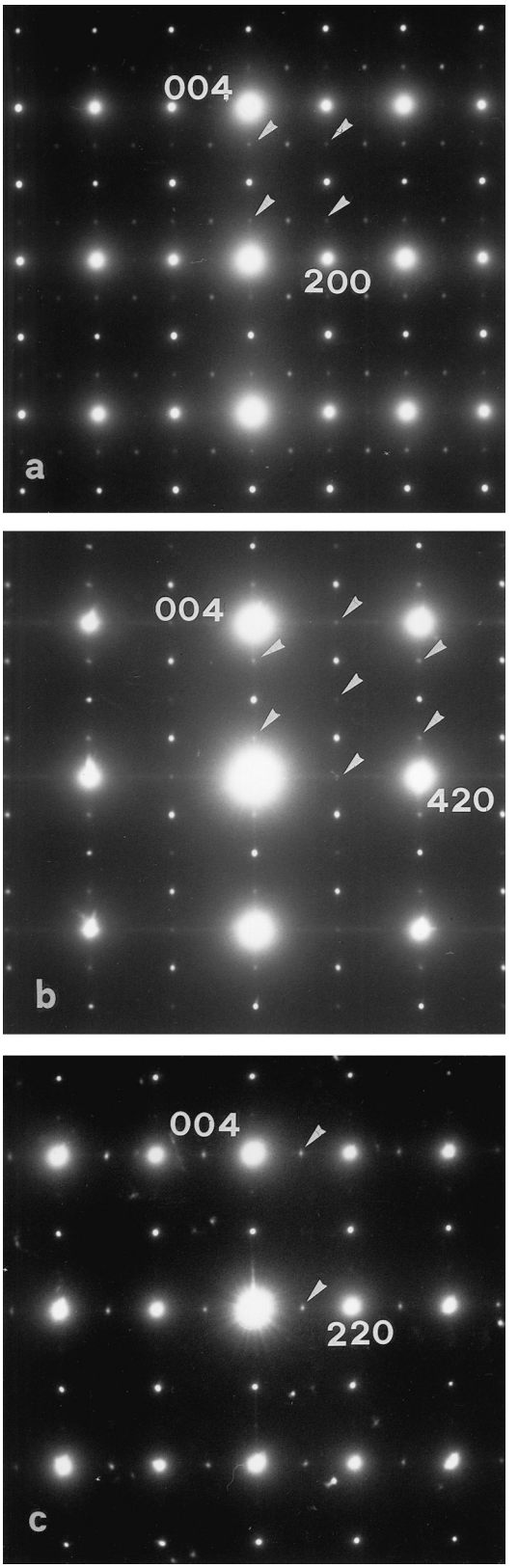

FIG. 2. Electron diffraction patterns along (a) $[010]_s$, (b) $[1\bar{2}0]_s$, and (c) $[1\bar{1}0]_s$ zone axes. Small arrows indicate the "reflections" which are caused from the streaking along the [010] direction.

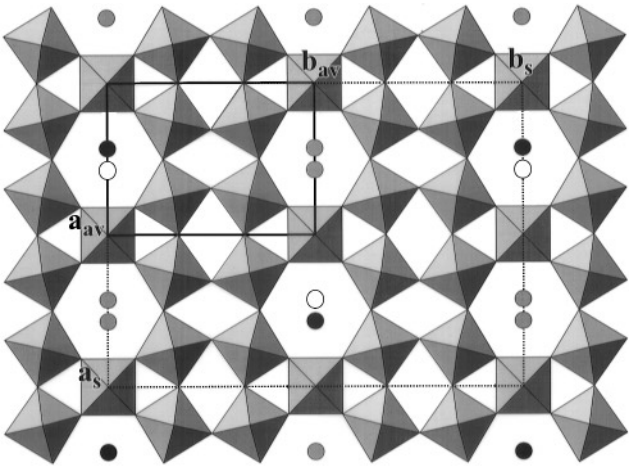

FIG. 3. Projection of the average structure of $Sb_{0.16}WO_3$ along the [001] direction showing the arrangement of the WO_6 octahedra and the positions of the Sb atoms (small circles inside the hexagonal tunnels). In the average structure all of the Sb sites are considered to be randomly occupied. In a partially ordered layer of the proposed superstructure model, the solid and open circles indicate the fully and partially occupied Sb sites, respectively.

streaking along the [010]* direction. The ED patterns along the $[1\bar{2}0]_s$ and $[1\bar{1}0]_s$ zone axes are shown in Figs. 2b and 2c, respectively. They also confirm the general reflection condition $h + k + l = 2n$. Unfortunately, despite our repeated attempts, we could not obtain ED patterns along the main zone axes [100] and [001]. Consequently, the exact space group assignment for the superstructure remains open. Our ED observations confirm only the body-centered lattice type of the superstructure. The observed streaking along the [010]* direction may be thought of as a result of random intergrowth of (010) slabs of differing structure types (*vide supra*) along the [010] direction. However, the appearance of the well-defined superstructure reflections shows that there are extended slabs, where some kind of structure modulation is present. Limiting ourselves to the results of the XRD study for the average structure we may consider the modulation of the sites occupation of the Sb atoms as the main reason for the formation of the observed superstructure. Such a structural model, consistent with the observed ED patterns, could be produced by introducing alternatively fully disordered and partially ordered (001) layers of WO_6 octahedra along the **c** axis. In a partially ordered (001) layer the fully occupied Sb sites are shown by the solid circles, while the randomly occupied Sb sites are shown with open circles (Fig. 3). This arrangement duplicates the unit cell along the $[100]_{av}$ and $[010]_{av}$ directions. A shifting of this layer by the vector $[112]_{av}$ leads to $c_s = 4c_{av}$ and produces a body-centered unit cell. Electron diffraction intensity calculations performed in the kinematical approximation and based on the above described structural model resulted in a good qualitative agreement with the observed ED patterns. Of course, more complex models cannot be excluded.

REFERENCES

1. M. Parmentier, A. Courtois, and C. Gleitzer, *C. R. Acad. Sci. Paris, Ser. C* **279,** 899 (1974).
2. M. Parmentier, C. Gleitzer, and A. Courtois, *Mater. Res. Bull.* **10,** 341 (1975).
3. T. Ekström, M. Parmentier, and R. J. D. Tilley, *J. Solid State Chem.* **34,** 397 (1980).
4. M. M. Dobson, J. L. Hutchison, R. J. D. Tilley, and K. A. Watts, *J. Solid State Chem.* **71,** 47 (1987).
5. S. R. Hall, H. D. Flack, and J. M. Stewart, "XTAL 3.2 Reference Manual." Universities of Western Australia, Geneva, and Maryland, 1992.
6. "International Tables for X-Ray Crystallography," Vol. IV. Kynoch Press, Birmingham, 1974.
7. (a) P. J. Becker and P. Coppens, *Acta Crystallogr. A* **30,** 129 (1974); (b) P. J. Becker and P. Coppens, *Acta Crystallogr. A* **30,** 148 (1974).
8. W. C. Hamilton, *Acta Crystallogr.* **18,** 502 (1965).
9. A. Hussain and L. Kihlborg, *Acta Crystallogr. A* **32,** 551 (1976).
10. L. H. Ahrens, *Geochim. Cosmochim. Acta* **2,** 155 (1952).
11. Ph. Labbé, M. Goreaud, B. Raveau, and J. Monier, *Acta Crystallogr. B* **34,** 1433 (1978).
12. M. Goreaud, Ph. Labbé, Y. Monfort, and B. Raveau, *Rev. Chim. Mineral.* **17,** 79 (1980).
13. S. T. Triantafyllou, P. C. Christidis, and Ch. B. Lioutas, *J. Solid State Chem.* [in press]